CONF-900704--9

DE90 009022

The Roles of PAH and Acetylene in Soot Nucleation and Growth

J. Thomas McKinnon[1] and Jack B. Howard

Department of Chemical Engineering
Massachusetts Institute of Technology
Cambridge, Massachusetts 02139

Subject Matter:

(24) Soot
(21) Pollutants
(1) Aerosols

FG02-84ER13282

Submitted to the Twenty-Third International Symposium on Combustion, University of Orleans, France, July 22-27, 1990.

Send correspondence to:

Professor J.B. Howard
Room 66-454
MIT, 77 Massachusetts Ave.
Cambridge, MA 02139
(617) 253-4574

[1]Present address:

TDA Research
Wheatridge, CO 80033

The Roles of PAH and Acetylene in Soot Nucleation and Growth

J. Thomas McKinnon and Jack B. Howard

Department of Chemical Engineering

Massachusetts Institute of Technology

Cambridge, Massachusetts 02139

Abstract

Soot nucleation and growth mechanisms involving PAH and C_2H_2 in distinct roles were quantitatively tested against experimental data including profiles of soot, PAH, C_2H_2 and other species present in flat benzene/oxygen/argon flames at 20 and 40 torr and equivalence ratios of 2.0, 2.125, and 2.4. In all the flames, the concentration of high molecular weight PAH was found to exhibit a maximum value near the onset of soot nucleation and to decline in the nucleation zone. A nucleation mechanism involving growth by reactive coagulation of heavy PAH in competition with destruction through OH attack gave good agreement between measured and predicted features of the soot nucleation kinetics. Conversely, soot nucleation through the growth of PAH by sequential addition of C_2H_2 with no PAH-PAH coagulation was much too slow to agree with data. PAH also contribute significantly to the post-nucleation growth of soot particles. Most of the mass of the soot system appears to come from C_2H_2 through the formation of the heavy PAH precursors to soot nuclei and the PAH that add to the growing soot particles, and direct C_2H_2 addition to the soot. Both the growth and oxidation reactions in these mechanisms are formulated as involving localized σ-radicals (i.e. aryl radicals in the case of PAH and active sites in the case of soot). The fraction of aryl radicals in the PAH and of active sites among carbon atoms of the soot surface are assumed to depend on a partial equilibrium involving the gas-phase concentration of H and H_2. The decrease in the surface growth rate of soot with time can be attributed in part to the decay in gas-phase concentration and a reduction in the hydrogen content of the soot.

Introduction

Soot nucleation and growth in flames occur in an environment rich in acetylene and polycyclic aromatic hydrocarbons (PAH). Acetylene has long been regarded as a dominant mass source for soot growth,[1] primarily because it is the most abundant hydrocarbon species in the sooting regions of a flame. A rate constant has been measured for the addition of C_2H_2 to soot surfaces[2]. PAH in sooting flames exhibit rise-and-decay concentration profiles peaking at later times for larger species, with decay of heavy PAH coinciding with soot nucleation.[3,4] Heavy PAH have long been proposed as soot intermediates (see reviews[5,6,7]), but without knowledge of whether these compounds produce soot nuclei by growing individually through mass addition from much smaller species or by also coagulating with each other.

Wersborg et al.[8] suggested M + M = S as a bimolecular reaction producing a soot nucleus S from two heavy hydrocarbons, M, and Bittner[3,9,10] obtained experimental evidence that heavy PAH are involved in soot nucleation. Recent modeling calculations by Frenklach[11], Colket et al.[12] and Harris and Weiner[13] have included PAH coagulation as particle inception.

The objective of this study was to clarify the roles of heavy PAH and C_2H_2 in soot nucleation and growth. To this end, concentration profiles of PAH, C_2H_2, and soot in several flames were measured, and soot nucleation and growth mechanisms were formulated and critically tested by comparing predicted kinetics against the data.

Experimental

Laminar premixed flat benzene/oxygen/argon flames were studied under the following sooting conditions (φ = equivalence ratio): 1) φ = 2.0, 20 torr, 30% Ar, 2) φ = 2.125, 40 torr, 45% Ar, and 3) φ = 2.4, 40 torr, 10% Ar. Condition 1 was selected to be similar to the flames studied by Bittner[9] [φ = 1.8 (almost sooting) and φ = 2.0)]. Condition 3 was selected to provide sufficient soot loadings for optical measurements. The

flames were stabilized on a water-cooled, perforated copper plate (12 mm thick) and surrounded by an annular non-sooting, C_2H_4/O_2 shield flame for lateral temperature uniformity. The burner chamber had several optical ports. Liquid benzene was metered with an HPLC syringe pump and vaporized in a temperature-controlled vessel. Gases (O_2, Ar, and C_2H_4) were metered with critical orifices.

Soot particle size, number density, and volume fraction were measured using standard laser scattering and absorption techniques[14]. Particle sizes were sufficiently small that the Rayleigh theory could be used to interpret the data. We used the optical properties of soot from Lee and Tien[15] and assumed a log-normal size distribution. Scattering measurements were made at 488 nm using a 3 watt argon-ion laser. Absorption measurements were made in the infrared at 1.4 μm to avoid absorption by PAH. Temperatures were determined in the $\varphi = 2.4$ flame using the brightness-emissivity method.[16,17]

PAH were measured by sampling flame gases from the flame using a water-cooled quartz probe with a 0.7 mm orifice.[16] The bottom 2 cm of the probe was uncooled to minimize flame perturbation. The pressure inside the probe was 1 torr or less for rapid expansion of the sample in the hot section. The heavy PAH (roughly 3 rings and larger) condensed on the probe walls while the lighter species were collected in a liquid-nitrogen trap ahead of the vacuum pump. The sample was extracted in dichloromethane (DCM) for analysis.

Light PAH (up to about 250 amu) were identified by capillary-column GC. The total amount of DCM soluble and insoluble material was determined gravimetrically.[18] The upper size limit of the DCM soluble PAH was estimated by fast-atom bombardment/mass spectrometry to be 900 amu. Light gases were sampled with a similar probe and analyzed with an on-line mass spectrometer.

Results

The PAH concentration profiles are shown in Figs. 1 and 2. Light solubles are larger than 2-rings but with an upper limit of about 5-rings (defined by the capillary GC). Soluble profiles for both flames exhibit slow growth followed by a rapid decline at the soot nucleation zone (see below). The profiles of insolubles for the two flames, however, are different. In the φ = 2.125 flame, the amount of insoluble material (M > 900 amu) formed is less than the total amount of PAH. Thus most of the intermediate PAH inventory was destroyed, either oxidized or pyrolyzed, rather than growing into insoluble material (soot). In the φ = 2.4 flame, the total amount of insoluble material rises to a value much larger than the peak amount of soluble material.

Fig 1
Fig 2

Figure 3 shows the profiles of soot number density, diameter and volume fraction along with temperature for the φ = 2.4, 40 torr flame. Diameter increases due to surface growth and coagulation while number density decreases due to coagulation. The line on the number density curve is predicted from the Smoluchowski equation,[19] (collision efficiency = 1). The volume fraction shows a rapid early climb followed by a leveling out.

Fig 3

Mass added to the soot could be either from PAH, C_2H_2, or both. Figure 4a shows the collision efficiency required if PAH were the only mass source for soot growth. The values greater than unity indicate that PAH cannot be a dominant source of mass for soot growth above 9 mm. Figure 4b shows the computed C_2H_2-soot surface growth rate constant[2] if C_2H_2 were the sole mass addition species. The decay in surface growth rate is similar to that of ref. 2.

Fig 4

Discussion

Possible mechanisms of soot nucleation and mass growth include 1) sequential addition of C_2H_2, and 2) reactive coagulation of PAH. Sequential addition of C_2H_2 to PAH is an extension of the mechanism which has been proposed.[3,4,9,20] If a soot nucleus is 2000 amu, then approximately 70 acetylene units would have to

be added to a small PAH molecule (e.g. phenanthrene). Reactive coagulation of PAH is an extension of the observation that young soot particles coagulate with sticking efficiencies near unity. If such a mechanism is operative for large molecular species, then only a few effective collisions would be required to form a soot nucleus.

Acetylene addition mechanism

The rate of acetylene addition to large PAH has not been measured, but can be estimated by extrapolating from both smaller and larger species. Fahr et al.[21] and Fahr and Stein[22] have measured a rate constant for the acetylene addition to phenyl radical forming phenylacetylene over the range 1000-1330 K, and Harris and Weiner[2] have determined a surface rate constant for acetylene addition to soot particles. These two processes may be mechanistically similar if addition to soot is the reaction of acetylene with localized σ-radicals or active sites[23] in the soot structure or on its surface. Because the σ-radical site is not delocalized over the π-electron network, its energy will not be a strong function of molecular size.[24]

The rate constants given in Table I are from ref. 21 and 22 where the authors stress that the data are taken over a narrow temperature range and that extrapolation is risky. However, due to the lack of any high temperature data we have computed rate constants at 1800 K, a typical temperature for soot nucleation in benzene flames. As can be seen from Table I, there is a 10-fold span in the rate constants which hopefully will bracket the actual value.

Also shown in Table I is the rate constant of ref. 2. In order to compare the rate expressions for acetylene + phenyl radical and acetylene + soot on the same basis, we have computed the collision efficiencies, or the ratio of the rate constant to the bimolecular collision rate, Z_{AB},

$$Z_{AB} = \pi\,[0.5(\sigma_A + \sigma_B)]^2 \left(\frac{8\,k_B T}{\pi\,\mu}\right)^{1/2} N_A\,N_B \qquad (1)$$

where σ_i is the collision (Lennard-Jones) diameter, k_B is the Boltzmann constant, μ is the reduced mass, and N_i is the number density of each colliding species.

For acetylene + phenyl radical the collision efficiency, η_{phenyl}, is described by,

$$\eta_{Phenyl} = \frac{k_{FMS}/N_{Av}}{\pi \sigma_{AB}^2 \left(\frac{8 k_B T}{\pi \mu_{AB}}\right)^{1/2}} \qquad (2)$$

where $k_{FS/FMS}$ is the rate constant from [21,22] and N_{Av} is Avagadro's number. For acetylene + soot surface the collision efficiency, η_{soot}, is given by,

$$\eta_{soot} = \frac{\frac{1}{M_{Ac}} k_{HW} \; 1000 \, R \, T}{\left(\frac{1}{2}\right)^2 \left(\frac{8 k_B T}{\pi \mu_{AB}}\right)^{1/2}} \qquad (3)$$

where M_{Ac} is the molecular weight of C_2H_2, k_{HW} is the rate constant from [2] and R is the gas constant.

As can be seen from Table I, the collision efficiencies for the two processes are similar, thereby supporting the concept that acetylene addition to phenyl radical and to soot involve similar mechanisms and that a generalized rate expression may be employed for the addition of acetylene to aryl radicals of any size.

The concept of soot nucleation through sequential addition of PAH can now be tested using Eq. 1, the above collision efficiency, and an acetylene mole fraction of 0.05, which is fairly typical of sooting flames.[3,9,25] The time required for growth from a small PAH, for example phenanthrene (178 amu), to a 2000 amu soot nucleus (i.e., the time to add 70 acetylenic units) is computed assuming the growing nucleus to be spherical with density 1.8 gm/cm^3. The measured time from the peak concentration of small PAH to the onset of yellow

luminosity is less than 1 ms.[3,9] The rate of growth of a particle under these conditions, expressed as the rate of increase of particle radius (r) is given by

$$\frac{dr}{dt} = \frac{\eta_{C_2H_2}}{4\rho}\left(\frac{8\,k_B\,T}{\pi\,m_{C_2H_2}}\right)^{1/2}\frac{(r_{C_2H_2}+r_{soot})^2}{r_{soot}^2}\,N_{C_2H_2}\,M_{C_2H_2} \qquad (4)$$

where η_{C2H2} is the C_2H_2-soot collision efficiency and ρ is the particle density. Integrating Eq. 4 from an initial seed PAH of radius r_o, we get

$$(r-r_o)+\frac{r_{C_2H_2}^2\,(r-r_o)}{(r_o+r_{C_2H_2})(r+r_{C_2H_2})}-2\,r_{C_2H_2}\,\ln\left(\frac{r+r_{C_2H_2}}{r_o+r_{C_2H_2}}\right)=\frac{\eta}{4\rho}\left(\frac{8\,k_B\,T}{\pi\,m_{C_2H_2}}\right)^{1/2}N_{C_2H_2}\,M_{C_2H_2}\,t \qquad (5)$$

If we take the Lennard-Jones diameter for phenanthrene (σ = 7.3 Å)[26] as $2r_o$ and the collision efficiency for soot (ref. 2) from Table I, Eq. 5 yields a time of 11 ms to produce a 2000 amu soot nucleus (r = 7.6 Å). This time is a lower limit, since oxidation is destroying the nucleus simultaneously with growth. Thus, the calculated time is more than 10-times greater than the observed time for the formation of soot nuclei.

Reactive Coagulation

Reactive coagulation refers to sticking collisions between PAH which are stabilized by the formation of a chemical bond. From Fig. 4a, the PAH-soot collision efficiency is 0.1-0.5 in the early part of the flame where PAH may dominate the soot mass growth. In our numerical modeling of nucleation,[25] we find the PAH-PAH collision efficiency, η_{PAH}, for heavy PAH to be in the range of 0.2 to 0.4 for to several flame conditions. Theoretical calculations of Miller[27] bracket η_{PAH} in this range. The measured concentration of heavy DCM solubles in the φ = 2.0, 20 torr, 30% Ar flame was 1.5×10^{-8} g/cm^3, and their average molecular weight is approximately 500 amu, considering the upper limit of the capillary GC (250 amu) and the solubility limit of PAH in DCM (900 amu). Thus the number density of heavy PAH is 1.8×10^{13} cm^{-3} and from Eq. 1, the time required to form a soot nucleus from these molecules, which takes only three effective collisions, is $(1/\eta)$ *

110 μs. Even if we use a lower η_{PAH} value of 0.2, the time required is within the observed limit of 1 ms.

Perhaps a more stringent test of the PAH coagulation concept is the comparison between coagulation rates and oxidation rates. The critical [PAH]/[OH] ratio at which the rate of mass removal from the oligomers by oxidation is balanced by the rate of mass addition through coagulation is given by

$$\frac{[PAH]}{[OH]} = \frac{\eta_{OH}}{\eta_{PAH}} \frac{[0.5\,(\sigma_{OH} + \sigma_{PAH})]^2}{0.5\,\sigma_{PAH}^2} \left(\frac{0.5\,M_{PAH}}{M_{OH}}\right)^{1/2} \frac{M_C}{M_{PAH}} \qquad (6)$$

where η_{OH} is the collision efficiency with which OH removes a carbon atom from soot and the 0.5 in the denominator avoids double counting PAH-PAH collisions.

From Neoh et al.[28], η_{OH} = 0.13 to 0.27. Bittner[3,9] measured $X_{OH} \approx 1x10^{-3}$ in the region of a benzene flame where the PAH are growing rapidly in size. He also observed the PAH concentration to change by a factor of 100 from φ = 1.8 (nearly sooting) to φ = 2.0 (lightly sooting). As shown in Table II, the predicted $[PAH]_{crit}$ falls between the observed experimental values in sooting and non-sooting flames, supporting the concept of soot nucleation as a competition between growth through reactive coagulation of PAH and destruction by oxidation. This approximate calculation ignores C_2H_2 addition which, as discussed below, is less significant than PAH addition in the nucleation zone.

The high molecular weight data of Bittner[3,9] further support reactive coagulation. The M>200 amu and M>700 amu concentration profiles each show a maximum at 8.1 mm and 10.0 mm above the burner (Fig. 5). At the flux maxima (9.1 mm and 10.3 mm) which occur slightly downstream of the concentration peak owing to diffusion, the formation reactions are just balanced by destruction reactions and the net rate is zero. From the measured C_2H_2 and OH concentrations, the ratio of the apparent collision efficiency for addition to that for oxidation (Table III) is 2.2 times greater at 10.3 mm than at 9.1 mm. The proposed mechanisms for C_2H_2

addition and OH oxidation are both by reaction with an aryl radical,[25] according to which the relative collision efficiencies would not be expected to vary with changes in OH and C_2H_2 concentrations. The observed increase in $\eta_{C_2H_2}/\eta_{OH}$ may indicate that the growth of the M>700 amu material is due to both C_2H_2 and M<700 PAH (reactive coagulation) with the relative contribution of the latter being larger at 9.1 mm where its concentration is large.

With the combination of reactive coagulation of PAH and surface reaction of C_2H_2, the apparent C_2H_2 surface growth rate measured in the benzene flame can be quantitatively interpreted. The data in Fig. 4b show a discontinuity at HAB = 7.5 mm, which corresponds closely to the point at which the PAH rapidly disappear. Thus, at HAB < 7.5 mm, the apparent C_2H_2 surface growth rate is very high because the mass addition to soot is not through C_2H_2 addition, but from PAH coagulation. At HAB ≥ 7.5 mm, most of the PAH has been removed from the flame by the soot, and the mass growth is due almost solely to C_2H_2 addition.

The decay in surface reactivity may also be interpreted using the model of acetylene plus an aryl radical. The surface density of aryl radicals (active sites) on the soot will be a function of hydrogen on the surface of the soot and the concentration of gas phase H atoms which can abstract the hydrogen. To a first approximation, the reaction

$$H + \begin{pmatrix}\text{PAH}\\ \text{Soot}\end{pmatrix} \rightarrow H_2 + \begin{pmatrix}\text{Aryl Radical}\\ \text{Soot w/ Active Site}\end{pmatrix} \qquad (7)$$

may be in equilibrium. Both the H/C ratio of the soot[29] and the H-atom concentration[3,9] are decreasing as mass is added to the soot system. Calculations[25] show that the product of these decay rates is comparable to the decay in surface reactivity.

Conclusions

The mass of the soot system can be described as coming from C_2H_2 through the growth of PAH that add to the soot and direct C_2H_2 addition to soot, but the addition of C_2H_2 to PAH is not itself sufficiently fast to account for the formation of 2000 amu soot nuclei. The reactive coagulation of heavy PAH, forming oligomers, with a collision efficiency in the range of 0.2 - 0.4 can account for the rate of appearance of soot nuclei.

This picture is supported by the observation that the earliest soot growth rates measured are too fast to be accounted for by C_2H_2 addition alone. At the point where the [PAH] has decayed to near zero the surface growth rate of soot has fallen close to a previously measured value.[2] The decrease in surface growth rate with time can be attributed to the decay in [H] and reduction in hydrogen content of the soot.

Acknowledgement

We are grateful to the Division of Chemical Sciences, Office of Basic Energy Research, Office of Energy Research, U.S. Department of Energy, for financial support under Grant Number DE-FG02-84ER13282.

References

1. Porter, G.: Fourth Symposium (International) on Combustion, p. 248, The Combustion Institute, 1953.

2. Harris, S.J. and Weiner, A.M.: Comb. Sci. Tech. 32, 267 (1983).

3. Bittner, J.D. and Howard, J.B.: Eighteenth Symposium (International) on Combustion, p. 1105, The Combustion Institute, 1981.

4. Bockhorn, H., Fetting, F., and Wenz, H.: Ber. Bunsenges Phys. Chem. 87, 1067, (1983).

5. Ray, S.K. and Long, R.: Comb. Flame 8, 139 (1964).

6. Lahaye, J., and Prado, G.: in Chemistry and Physics of Carbon, Vol. 14, (P.L. Walker and P.A. Thrower, Eds.), p. 168, Marcel Dekker, New York, 1978.

7. Haynes, B.S., and Wagner, H.Gg.: Prog. Energy Comb. Sci. 7, 229 (1981).

8. Wersborg, B.L., Yeung, A.C., and Howard, J.B.: Fifteenth Symposium (International) on Combustion, p. 1439, The Combustion Institute, 1975.

9. Bittner, J.D.: A Molecular Beam Mass Spectrometer Study of Fuel-Rich and Sooting Benzene-Oxygen Flames, Ph.D. thesis, Department of Chemical Engineering, Massachusetts Institute of Technology, 1981.

10. Howard, J.B. and Bittner, J.B.: in Soot in Combustion Systems and Its Toxic Properties, (J. Lahaye and G. Prado, Eds.), p. 57, Plenum Press, New York, 1983.

11. Frenklach, M.: Detailed Modeling of Soot Particle Nucleation and Growth, Poster 26, Twenty-Second Symposium (International) on Combustion, The Combustion Institute, 1988.

12. Colket, M.B., Hall, R.J., Sangiovanni, J.J., and Seery, D.J.: The Determination of Rate-Limiting Steps during Soot Formation. Report No. UTRC89-13, United Technologies Research Center, East Hartford, Conn., 1989.

13. Harris, S.J., and Weiner, A.M.: Twenty-Second Symposium (International) on Combustion, p. 333, The Combustion Institute, 1988.

14. D'Alessio, A., Di Lorenzo, A., Sarofim, A.F., Beretta, F., Masi, S., and Venitozzi, C.: Fifteenth Symposium (International) on Combustion, p. 1427, The Combustion Institute, 1975.

15. Lee, S.C. and Tien, C.L.: Eighteenth Symposium (International) on Combustion, p. 1159, The Combustion Institute 1980.

16. Fristrom, R.M. and Westenberg, A.A., Flame Structure, McGraw-Hill, New York, 1965.

17. D'Alessio, A., Beretta, F., and Venitozzi, C.: Comb. Sci. Tech. 5, 263 (1972).

18. Lafleur, A.L., Monchamp, P.A., Plummer, E.F., and Kruzel, E.L.: Anal. Let. 19, 2013 (1986).

19. Prado, G., Lahaye, J., and Haynes, B.S.: in Soot in Combustion Systems and Its Toxic Properties, (J. Lahaye and G. Prado, Eds.), p. 145, Plenum Press, New York, 1983.

20. Frenklach, M., Clary, D.W., Gardiner, W.C., and Stein, S.E.: Twentieth Symposium (International) on Combustion, p. 887, The Combustion Institute, 1984.

21. Fahr, A., Mallard, W.G., and Stein, S.E.: Twenty-First Symposium (International) on Combustion, p. 825, The Combustion Institute, 1986.

22. Fahr, A., and Stein, S.E.: Twenty-Second Symposium (International) on Combustion, p. 1023, The Combustion Institute, 1988.

23. Coulson, C.A.: Proc. Fourth Conf. on Carbon, p. 215, Pergamon Press, 1960.

24. Chen, R.H., Kafafi, S.A., and Stein, S.E.: J. Am. Chem. Soc. 111, 1418 (1989).

25. McKinnon, J.T. and Howard, J.B.: Comb. Flame (to be submitted), 1990.

26. Pope, C.J.: Fluxes and Net Reaction Rates of High Molecular Weight Material in a Near-Sooting Benzene-Oxygen Flame, M.S. Thesis, Department of Chemical Engineering, Massachusetts Institute of Technology, 1988.

27. Miller, J.H.: Twenty-Third Symposium (International) on Combustion, (submitted), The Combustion Institute, 1990.

28. Neoh, K.G., Howard, J.B., and Sarofim, A.F.: in Particulate Carbon Formation During Combustion, (D.C. Siegla and G.W. Smith, Eds.), p. 261, Plenum Press, New York, 1981.

29. Homann, K.H., and Wagner, H.Gg.: Eleventh Symposium (International) on Combustion, p. 371, The Combustion Institute, 1967.

Figure Captions

Figure 1. Profiles of PAH from φ = 2.125, 45% Ar, 40 torr flame. Circles - Light DCM soluble material representing material from 128 to 250 amu. Triangles - Total DCM solubles: 128 amu to 900 amu. Squares - Total material collected, DCM soluble + insoluble.

Figure 2. Profiles of PAH for φ = 2.4, 10% Ar, 40 torr flame. Circles - Total DCM solubles: 128 amu to 900 amu. Triangles - Total material collected, soluble + insoluble.

Figure 3. Soot particle dynamics and temperature profiles for φ = 2.4, 10% Ar, 40 torr flame. Triangles - Number density, line represents prediction from Smoluchowski equation. Circles - Diameter. Diamonds - Volume fraction. Squares - Temperature. Shift profiles 3 mm away from burner to compare to probe sampling measurements.

Figure 4. a) Required collision efficiency between PAH and soot if all mass addition to soot comes from PAH. b) Surface growth rate constant for soot (per unit partial pressure of C_2H_2) if all mass addition to soot comes from acetylene, computed as in ref. 2.

Figure 5. PAH profiles from Bittner[9,10]. Solid line represents all material of M > 200 amu. Dashed line is for M > 700 amu.

Table Captions

Table I. Comparison of rate constants for acetylene addition to phenyl radical and acetylene to soot. Collision efficiency, η, computed at 1800 K. Phenyl + C_2H_2 rate constants: A) from ref. 21, B) taken from figure in ref. 22 representing data of ref. 21, C) recommendation from ref. 22.

Table II. Calculated critical concentration of PAH relative to experimental non-sooting and sooting measurements given that: $X_{OH} = 1x10^{-3}$ for $\varphi = 1.8$ and 2.0, $\eta_{PAH} = \eta_{OH} = 0.2$. X_{OH} is believed to be a weak function of φ.

Table III. Comparison of the apparent ratio η_{C2H2}/η_{OH} at two points in Bittner[3,9] flame given measured OH and C_2H_2 concentrations.

Table I.

		Rate Constant	k_{1800}	η x10^3
$C_2H_2 + C_6H_5 \rightarrow$	(A)	$10^{11.5}$ exp(-1.4/RT)	$2.1x10^{11}$	0.43
$C_6H_5C_2H + H$	(B)	$10^{9.5}$ exp(-5.5/RT)	$7.5x10^{11}$	1.54
Rate = $k[C_2H_2][C_6H_5]$	(C)	$10^{13.6}$ exp(-10.1/RT)	$2.3x10^{12}$	4.71
		units: mol/cm^3 s, kcal/mol		
C_2H_2 + Soot		$3.0x10^{-3}$ @ max	$3.0x10^{-3}$	0.59
Rate = k S P_{C2H2}		units: gm/s cm^2 atm		

Table II.

Calculated Condition		[PAH] cm^{-3}
$\tau_{ox} = \tau_{coag}$	Calculated critical sooting [PAH]	$8.3x10^{12}$
Experimental Conditions		
φ = 1.8	Non-sooting	$1.8x10^{12}$
φ = 2.0	Lightly sooting	$1.8x10^{13}$

Table III.

	Peak Flux, M>200	Peak Flux, M>700
HAB (mm)	9.1	10.3
X_{OH}	$9.5x10^{-4}$	$1.5x10^{-3}$
X_{C2H2}	$4.8x10^{-2}$	$3.7x10^{-2}$
η_{C2H2}/η_{OH}	$1.1x10^{-2}$	$2.37x10^{-2}$

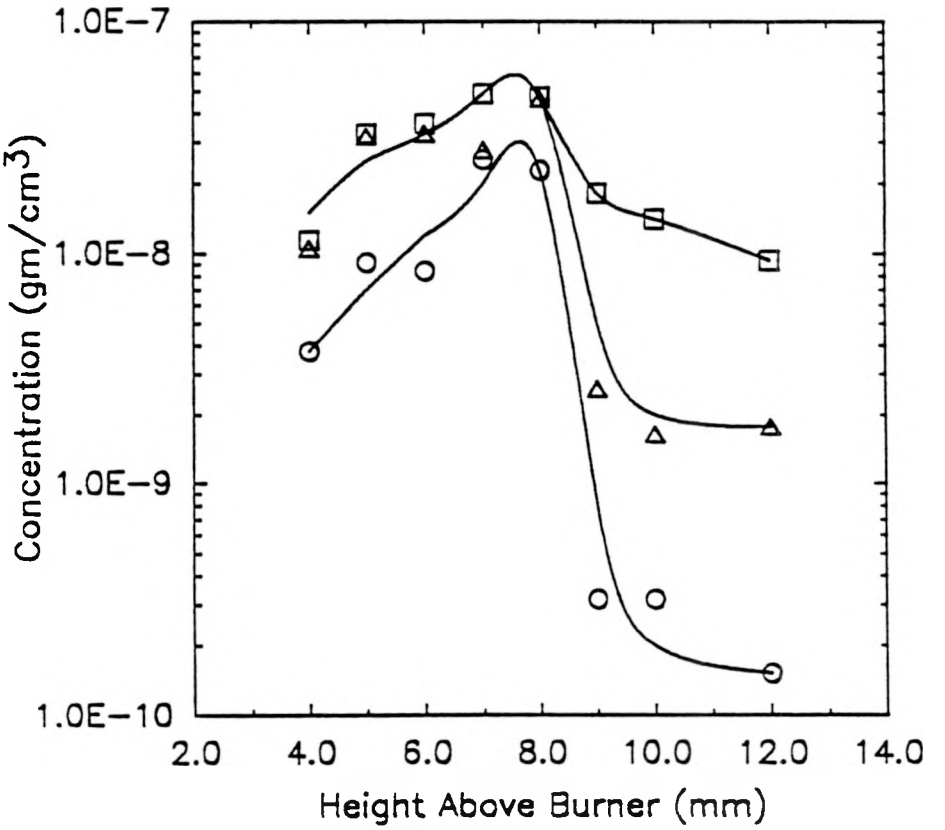

Figure 1. Profiles of PAH from φ = 2.125, 45% Ar, 40 torr flame. Circles - Light DCM soluble material representing material from 128 to 250 amu. Triangles - Total DCM solubles: 128 amu to 900 amu. Squares - Total material collected, DCM soluble + insoluble.

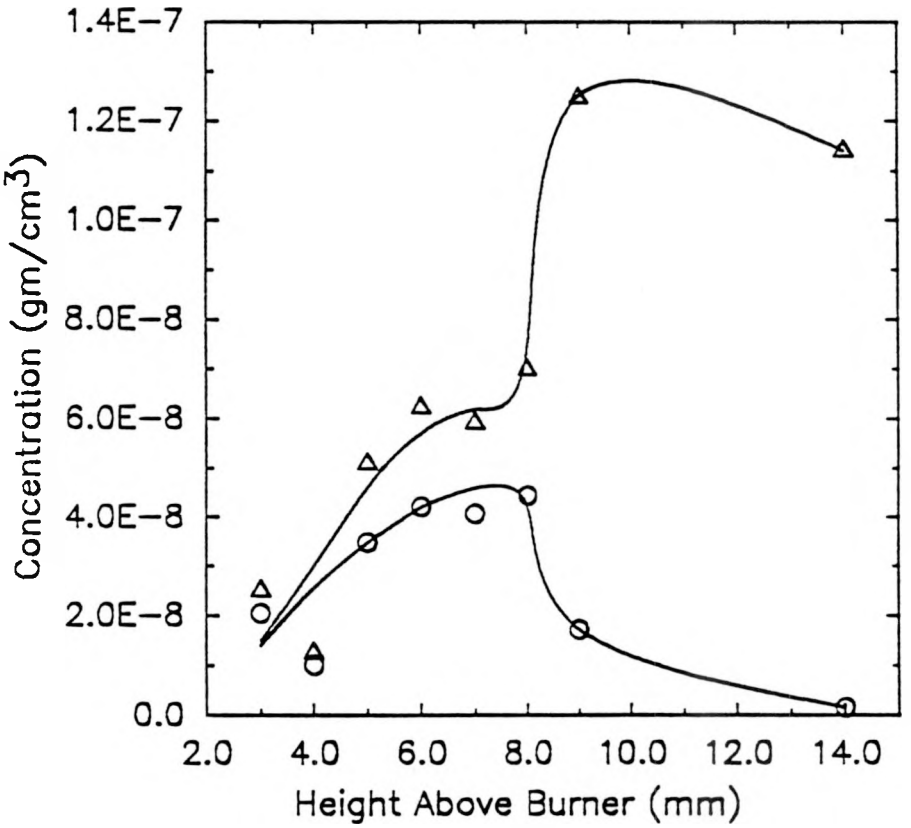

Figure 2. Profiles of PAH for φ = 2.4, 10% Ar, 40 torr flame. Circles - Total DCM solubles: 128 amu to 900 amu. Triangles - Total material collected, soluble + insoluble.

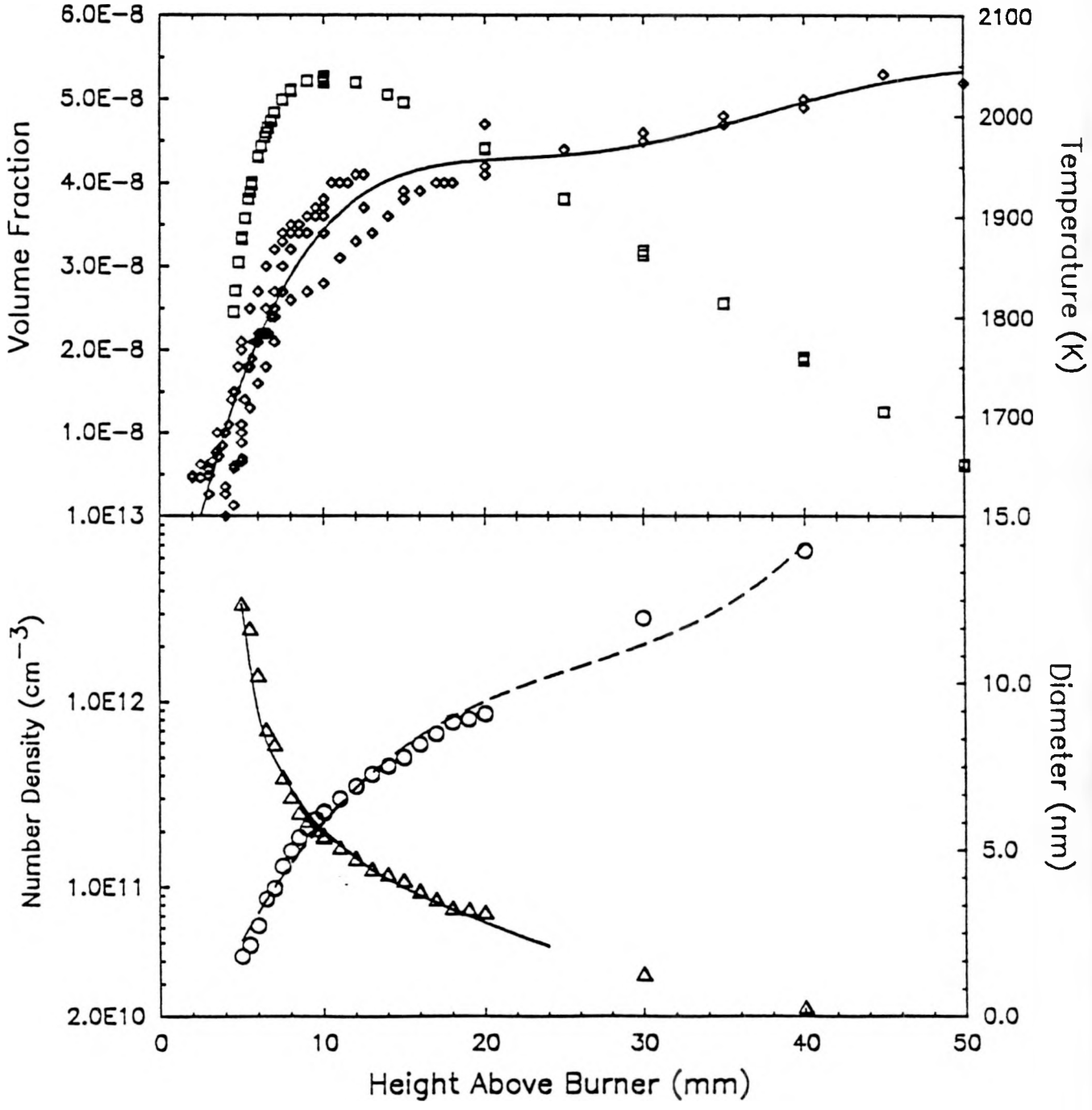

Figure 3. Soot particle dynamics and temperature profiles for φ = 2.4, 10% Ar, 40 torr flame. Triangles - Number density, line represents prediction from Smoluchowski equation. Circles - Diameter. Diamonds - Volume fraction. Squares - Temperature. Shift profiles 3 mm away from burner to compare to probe sampling measurements.

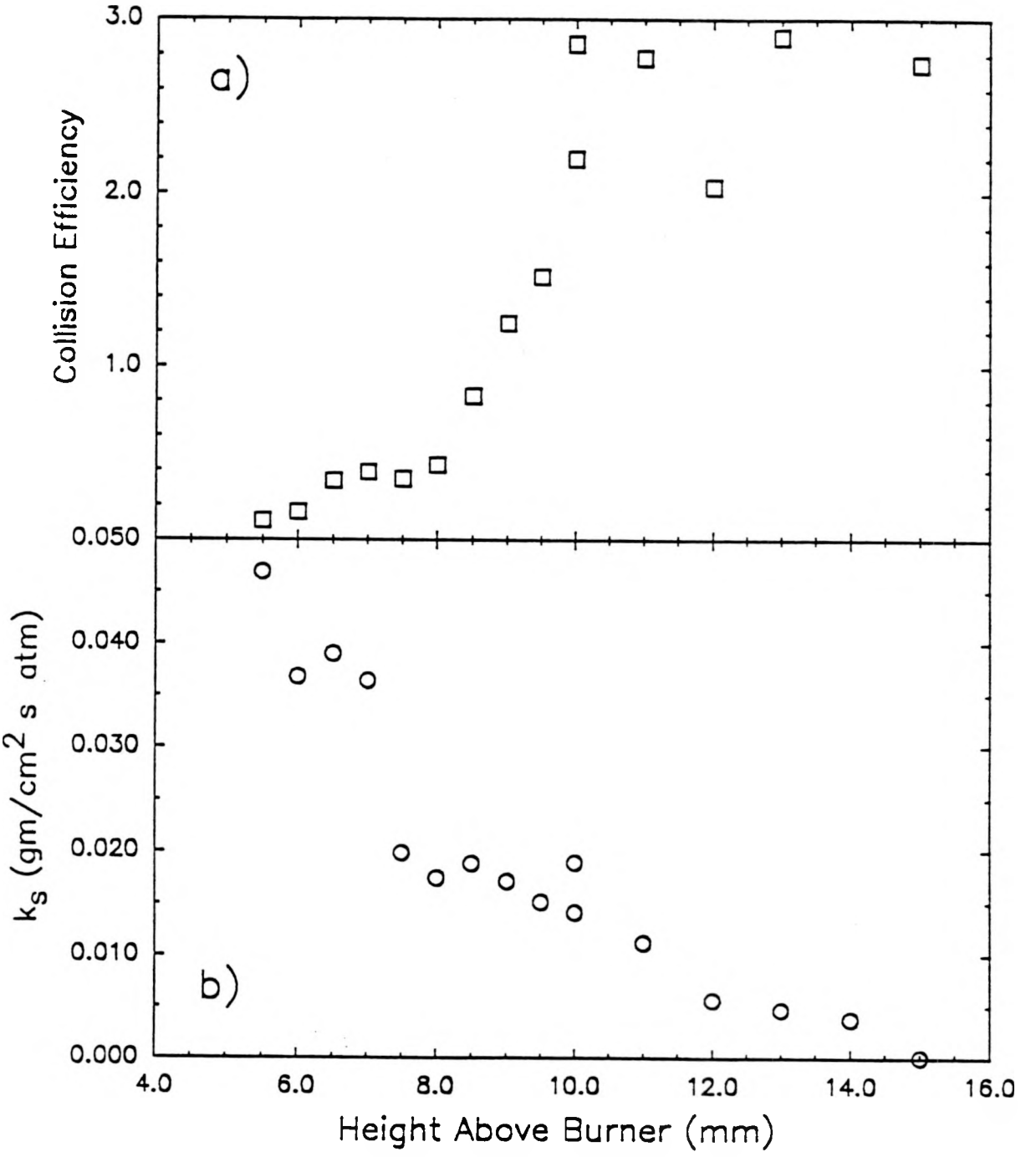

Figure 4. a) Required collision efficiency between PAH and soot if all mass addition to soot comes from PAH. b) Surface growth rate constant for soot (per unit partial pressure of C_2H_2) if all mass addition to soot comes from acetylene, computed as in ref. 2.

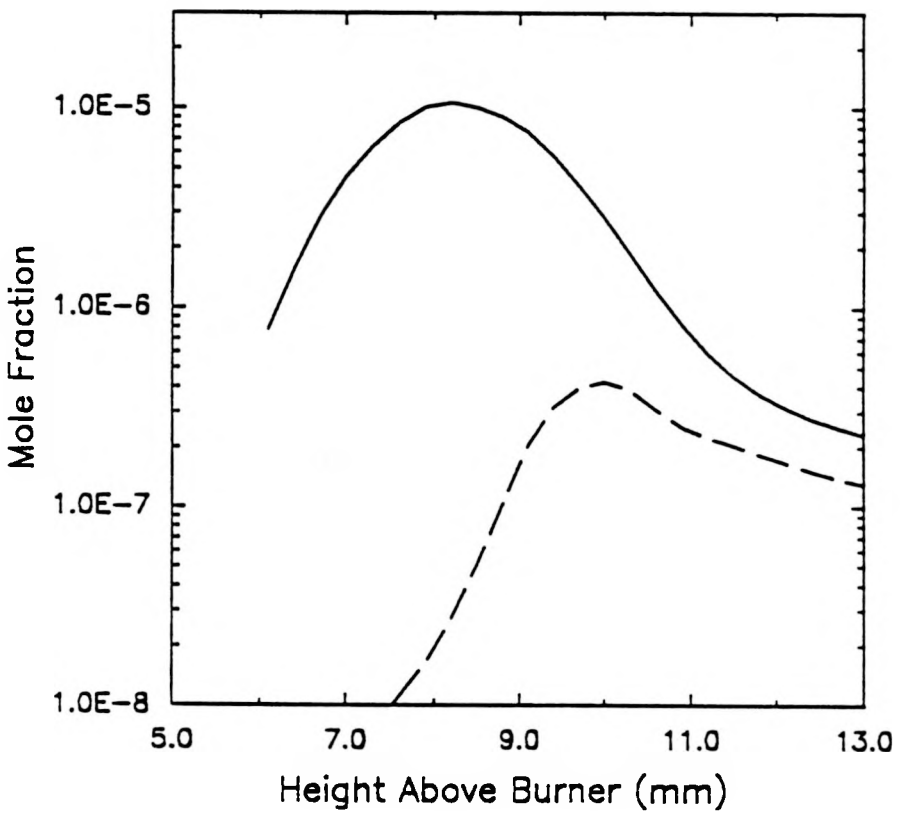

Figure 5. PAH profiles from Bittner[9,10]. Solid line represents all material of M > 200 amu. Dashed line is for M > 700 amu.